

2  
3 **The sunny side of the Ice Age: Solar insolation as a potential long-term pacemaker for**  
4 **demographic developments in Europe between 43 and 15 ka ago**

5  
6 Andreas Maier<sup>1\*</sup>, Patrick Ludwig<sup>2</sup>, Andreas Zimmermann<sup>1</sup> & Isabell Schmidt<sup>1</sup>

7  
8  
9 University of Cologne, Institute of Prehistoric Archaeology, Collaborative Research Centre 806, Bernhard-  
10 Feilchenfeld-Str. 11, 50969 Cologne, Germany.

11  
12 Institute of Meteorology and Climate Research - Department Troposphere Research; Regional Climate and  
13 Weather Hazards; Karlsruhe Institute of Technology. Wolfgang-Gaede-Strasse 1, 76131 Karlsruhe, Germany.

14  
15 [\\*a.maier@uni-koeln.de](mailto:a.maier@uni-koeln.de)

16  
17 **ABSTRACT**

18 After a decade of research under the auspices of the project 'Population dynamics: Land use  
19 patterns of populations between the Upper Pleistocene and Middle Holocene in Europe and  
20 the Middle East', a consistent sequence of high-resolution palaeodemographic datasets has  
21 been compiled, spanning the entire Upper Paleolithic from roughly 43 to 15 ka ago. When  
22 viewed in a diachronic perspective, long-term trends of increasing and decreasing population  
23 sizes and densities, as well as expanding and contracting areas of settlement activities (Core  
24 Areas) become evident. An environmental parameter with potentially strong impact on  
25 hunter-gatherers societies is solar insolation. The sun's energy available at a certain time  
26 and place is one of the main factors influencing plant growth. The amount of plant biomass,  
27 in turn, largely determines the amount of animal biomass in a landscape. The latter is the  
28 most important source of energy for European Upper Palaeolithic hunter-gatherers. Here, we  
29 aim to assess the potential influence of changes in solar insolation on palaeodemographic  
30 development in Western and Central Europe between 43 and 15 ka ago. To this end, we  
31 present estimates on the number, density and spatial distribution of hunter-gatherers for five  
32 consecutive Upper Paleolithic periods in Europe. Based on regional climate model data for  
33 the Last Glacial Maximum and solar insolation data, we calculate (1) differences in the  
34 amount of Megajoule per square meter (MJm<sup>-2</sup>), (2) start, end, and length of the growing  
35 season, as well as (3) summed temperatures during the entire duration and during the first  
36 30 days of the growing season. A comparison shows that a moderate, steady increase of  
37 population size and an extension of the Core Areas between 43 and 29 ka coincides with an  
38 increase in the summed temperature, particularly during the first 30 days of the growing  
39 season. The period between 29 and 25 ka shows a pronounced population decline, a strong  
40 contraction of Core Areas and a withdrawal from higher latitudes. This coincides with a  
41 markedly delayed growing season, a decrease in summed temperatures, and a marked  
42 reduction in solar insolation during the early part of the growing season. Between 25 and 20  
43 ka, we see consolidation and renewed growth in both numbers and densities of people and  
44 an expansion and merging of Core Areas in Western Europe. There is a slight gain in the  
45 energy available during the first half of the year. The growing season starts earlier and is of  
46 increasingly longer duration, coupled with rising summed temperatures. Between 20 and 15  
47 ka, the meta-population grows strongly, Core Areas expand and the higher latitudes become  
48 repopulated. This coincides with further increasing summed temperatures and an ever-earlier  
49 start to the growing season. Additionally, the gain in available solar energy during the early  
50 phase of the growing season is particularly pronounced. These findings indicate that solar  
51 insolation and its effects on an ecosystem's phenological configuration over different trophic  
52 levels is indeed an important factor in the long-term demographic development of Paleolithic  
53 hunter-gatherers.

54  
55 **Key words:** Palaeodemography, Upper Palaeolithic, Solar Insolation, Phenology, Growing  
56 Season, biomass production

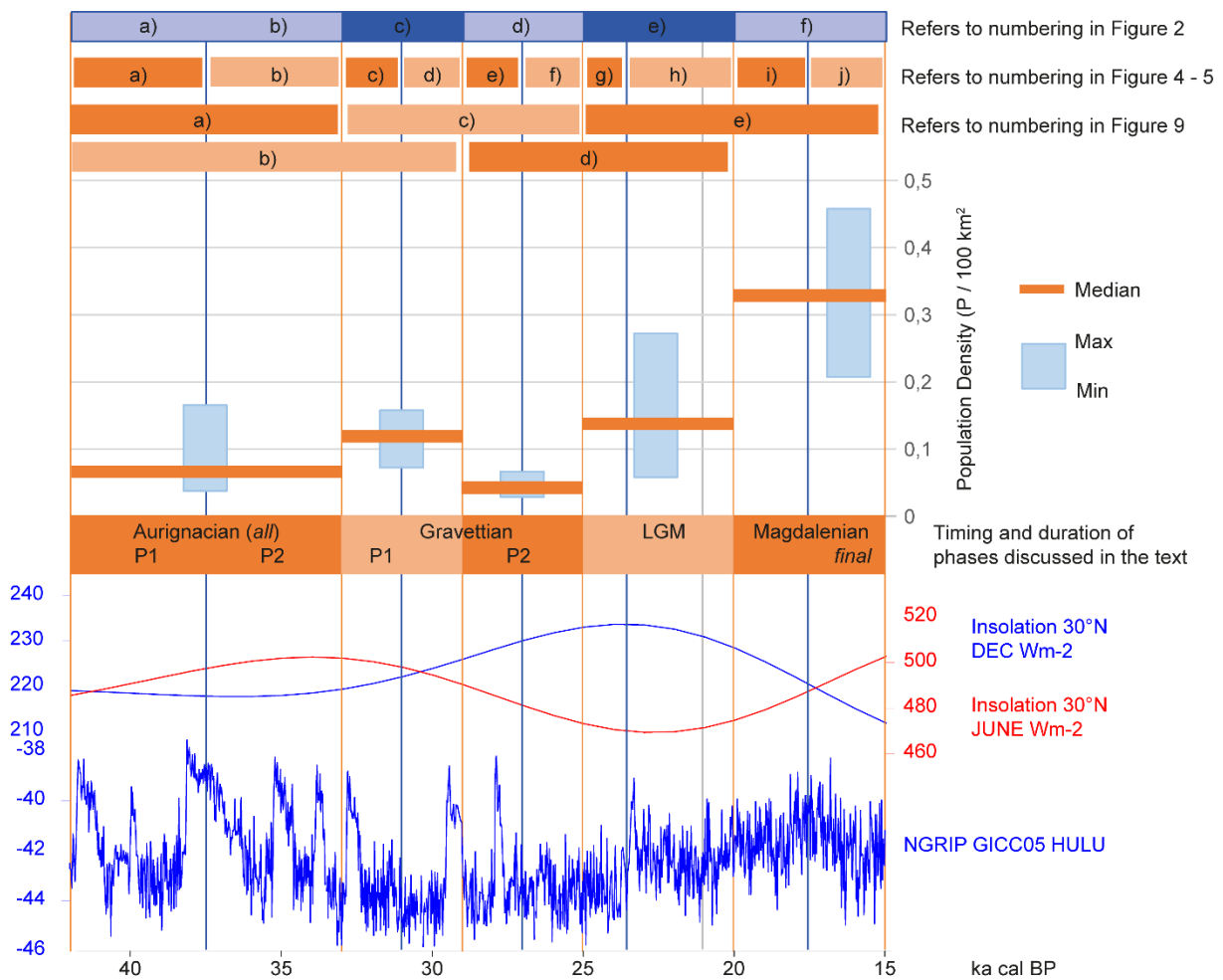
## 1. INTRODUCTION

Over the last two decades, several innovative approaches to paleodemography (Bocquet-Appel and Demars 2000; Bocquet-Appel et al. 2005; French 2015; French and Collins 2015; Kretschmer 2015; Maier et al. 2016; Maier and Zimmermann 2017; Schmidt and Zimmermann 2019; Tallavaara et al. 2015) and population genetics (e.g. Fu et al. 2016; Posth et al. 2016) have advanced research on Upper Palaeolithic population dynamics. At the same time, a number of factors have been discussed with regard to their explanatory potential for the observed demographic developments; these include technological gain and loss, social organisation and norms, and environment (Boserup 1965; Bradtmöller et al. 2010; French 2018; Gamble 2002; Gamble et al. 2004; Henderson and Loreau 2019; Roebroeks 2006). To be clear, social and technological factors certainly play an important role in human population dynamics and innovations or a loss of technological knowledge can affect population dynamics strongly. However, for large-scale studies such as this one, there are two major problems for exploring their impact on the number, density and distribution of humans in a landscape. The first problem is that social, technological, and demographic developments are interdependent, where social organisation may influence demographic developments and vice versa. Thus, it is extremely difficult to distinguish cause from effect. The second problem is that social organisation and technological repertoires depend on human decision making, which is observable at a different timescale than long-term developments. Long-term demographic developments over the period of several millennia are incompatible with human decision-making. Environmental change, on the other hand, can be meaningfully observed at small and large temporal scales. The impact of human societies on the environment during the Palaeolithic is subject to debates. Topics range from reflections on negative impacts on forest cover (Kaplan et al. 2016) to the involvement in the extinction of larger animals (e.g. Koch and Barnosky 2006; Sandom et al. 2014). However, during the entire period of observation between 43 and 15 ka, human influence on environment and particularly on climate seems to have been comparatively small, making it relatively easy to distinguish between cause and effect. Nonetheless, proving a causal relationship remains difficult, not least because of incompatible or insufficient temporal and spatial resolution in the archaeological data. The introduction of absolute numbers and densities of human populations as a new, quantified variable at a comparatively high spatial and temporal resolution is a first step in addressing this problem. While acknowledging the importance of social and technological factors for demographic developments, this paper will focus on environmental change and its explanatory potential for the changes we observe in the currently available palaeodemographic data.

The data for successive time-slices (Kretschmer 2015; Maier et al. 2016; Maier and Zimmermann 2017; Schmidt and Zimmermann 2019), has a temporal resolution of between 4 and 5 ka. Temperature change, as captured in the ice-core records, varies at a frequency much too high to be meaningfully compared to our data (**Figure 1**). Moreover, low temperatures alone are not a limiting factor for human settlement activities. To the contrary, it has been shown that some Palaeolithic hunter-gatherer communities preferred permafrost over equally accessible non-permafrost areas (Demidenko 2018; Maier et al. 2016). However, it would be overstated to assume that environmental thresholds were virtually meaningless for well-adapted Palaeolithic hunter-gatherers. Rather than temperature alone, the availability of animal biomass was probably a key factor to allow permanent settlement in a region (Kelly 1983; Mandryk 1993). The amount and diversity of animal biomass, in turn, is dependent on the amount and quality of primary plant biomass (Olf et al. 2002). A very important factor for the production of plant biomass is solar insolation (Monteith 1994). At the same time, this environmental parameter changes gradually and slowly, making it compatible to our demographic estimates (**Figure 1**). Solar insolation affects plant biomass production in two primary ways. Firstly, it drives air temperatures near the surface, one of the main factors determining the length of the growing season (Jiang et al. 2018). This correlation is so strong that temperature-based models to estimate insolation perform better than those based on sunshine, particularly when averaged to a monthly base (Hassan et al. 2016). Secondly, it provides the energy needed for photosynthesis and there is a linear relationship between

114 solar insolation and biomass production (Gosse et al. 1986). Therefore it seems to be an  
 115 important factor in an ecosystem's phenological configuration, i.e. in the timing of periodic life  
 116 cycle parameters of plants and animals (Gienapp et al. 2014; Parmesan and Hanley 2015;  
 117 Liu et al. 2016, Huang et al. 2019). Phenological shifts may be effective over different trophic  
 118 levels and lead to mismatches in resource availability and predator-prey relations (Burrows et  
 119 al. 2011; Ohlberger et al. 2014). It has been shown for birds that these mismatches affect  
 120 migrating species particularly strong when an expected food resource is not available upon  
 121 arrival (Both et al. 2010; Mayor et al. 2017).  
 122 In the following, we will evaluate estimates of the number and density of people as well as  
 123 the position and extent of Core Areas against insolation data for the period between 40 ka  
 124 and 15 ka.

125  
 126  
 127



128  
 129  
 130  
 131  
 132  
 133  
 134  
 135  
 136  
 137  
 138  
 139  
 140  
 141  
 142

**Figure 1: Overview on timeframe and temporal scales of data.** Population density estimates are given for the generalised Total Area of Calculation (TAC) of 2.3 Million km<sup>2</sup> (see **Figure 2** for spatial extent), terminology for archaeological phases corresponds with **Table 1**. Note: estimates for the Magdalenian in total have not been calculated (see Kretschmer 2015), but would resemble those of the Final Magdalenian. Vertical lines indicate "insolation reference dates": Blue lines indicate Insolation values used for synchronic illustrations (**Figure 2**), orange lines for calculating differences in insolation for diachronic developments (**Figure 9**), grey line at 21ka indicates anchor point of the PMIP3 LGM climate model data. Timeframes covered in **Figure 2** and **9** are indicated and labelled accordingly. Insolation (30° N, June and December) and GISP 2 Delta18O/16O are taken from Climate Data CalPal (Weninger and Jöris 2008, accessed 27.06.2019).

## 2. MATERIAL AND METHODS

### 2.1 PALEODEMOGRAPHIC AND SPATIAL DATA

The study uses spatial information on site locations and raw material transport as well as derived demographic data for the periods of 42-33 ka (Aurignacian, Schmidt and Zimmermann 2019), 33-29 ka and 29-25 ka (Gravettian subdivided into an early phase 1 and later phase 2, Maier and Zimmermann 2017), 25-20 ka (LGM, Maier et al. 2016), and 20-14 ka (Magdalenian, Kretschmer 2015). The approach to estimate population sizes and densities, the “Cologne Protocol”, was developed and described for Neolithic and younger periods (Zimmermann et al. 2009) and subsequently transferred to hunter-gatherer contexts (Kretschmer 2015). For details on the protocol, we refer the reader to Maier et al. (2016) and the supplementary material of Maier and Zimmermann (2017). Briefly, the protocol distinguishes areas of intensive use, so-called Core Areas, from areas which have been used either ephemerally, temporarily (e.g. during short phases of perceived climatic amelioration) or even not at all. Core Areas thus provide the minimum, but also the most robust evidence for human presence on a large spatial *and* temporal scale (e.g. Klein et al. In prep.). Core Areas are modelled within a defined map section, called Total Area of Calculation (TAC). The spatial distribution of Core Areas and the TAC used for the European Upper Palaeolithic is given in **Figure 2**. In a next step, spatial information on lithic raw material transport is used to estimate the number of groups within a Core Area. Using information on group sizes from the ethnographic literature, number and density of people within a Core Area and within the TAC are inferred. **Table 1** reviews the basic data for the paleodemographic estimates. For the Magdalenian we used data from the final Magdalenian period only, instead of averaging the higher resolution data provided by Kretschmer (2015). Similarly, for reasons of comparability, the demographic density estimates presented in **Table 1** are calculated based on a unified TAC, comprising 2,300,000 km<sup>2</sup> and illustrated in **Figure 2**, thus partially differing from previously published estimates. Core Areas for the final Magdalenian located outside the TAC (e.g. in Great Britain and Italy) were not considered for calculating spatial differences in Core Area distributions.

### 2.2 ENVIRONMENTAL DATA

Insolation data after Berger (1978) in Watt per square meter (Wm<sup>-2</sup>) was obtained from the R package palinsol (Crucifix 2016) for twelve successive “insolation reference dates” at 42, 37.5, 33, 31, 29, 27, 25, 23.5, 21, 20, 17, and 15 ka cal BP (see **Figure 1**). These insolation reference dates were chosen to coincide with the boundaries and midpoints of the periods for the palaeodemographic estimates to provide an optimal fit of the data (**Figure 2**). The only exception is the LGM period, for which two internal insolation reference date are provided. This accounts for the observation of the transition between the Solutrean and Badegoulian in the archaeological record at around 23.5 ka as well as for the anchor point of our climatic data at 21ka, which is the focus time of the PMIP3 (Paleoclimate Modelling Intercomparison Project, Phase 3, Braconnot et al. 2012) LGM climate models (21 ka). Averaged daily temperatures (2 meters above ground level) were obtained from a 30 year long regional climate model simulation (horizontal grid spacing ~50km) with the WRF model (Weather Research and Forecasting, Skamarock et al. 2008) that was nested into the coarse gridded (~200 km horizontal grid spacing) MPI-ESM-P (Max Planck Institute for Meteorology Earth System Model in Paleo model, Giorgetta et al. 2013) LGM simulation. The regional WRF model has been adapted to LGM boundary conditions (e.g. ice sheets, lowered sea level, orbital parameters) and is forced by 6-hourly MPI-ESM-P data at its lateral boundaries (Ludwig et al. 2017). Additionally, an adjustment of sea surface temperatures based on the MARGO project (Multiproxy Approach for the Reconstruction of the Glacial Ocean surface, MARGO Project Members 2009) yield a better agreement of the WRF model results with the available proxy data (Ludwig et al. 2017). For comparison with the present-day, an additional WRF simulation has been performed that was forced by MPI-ESM-P data for present day climate simulation.

198 In order to transform these data into information meaningful for the production of primary  
199 biomass, we estimate for each insolation reference date the available energy per month at a  
200 given latitude in Megajoule per square meter ( $MJm^{-2}$ ), as well as the start, end, length, and  
201 summed temperature of the growing season.

202 To transfer monthly  $Wm^{-2}$  into monthly  $MJm^{-2}$  we use the following function

$$203 \quad MJm^{-2}_{month} = \left( \frac{Wm^{-2}}{1000} \right) \times ld_{lat} \times nd \times 3.6$$

204 where  $ld_{lat}$  is the length of daylight at a given latitude under current orbital conditions,  $nd$  is  
205 the number of days per month and 3.6 is the factor to transform kWh into MJ. Given the large  
206 scale of this study, we ignore insolation distortions introduced by local topography or daily  
207 differences due to cloud cover.

208  
209 By most definitions, the growing season starts with six consecutive days of a mean daily  
210 temperature near the surface above  $5^{\circ}C$  and ends with six consecutive days below  $5^{\circ}C$  of  
211 mean daily temperature (Jiang et al. 2018). Since mean daily temperatures in the model data  
212 are averaged over 30 years, increases and decreases are rather steady and reversions are  
213 rare. In order to account for this increased steadiness, we calculated the length of the  
214 growing season as the number of days between the first of the first three consecutive days  
215 above  $5^{\circ}C$  and the last day before the first three consecutive days below  $5^{\circ}C$ .

216  
217 In order to estimate the start, end, and length of the growing season at  $50^{\circ}N$  and  $45^{\circ}N$  for  
218 each of the twelve insolation reference dates, we used the finding by Van Meerbeeck et al.  
219 (2009: 44) that during MIS 3 an increase in  $4 Wm^{-2}$  resulted in an increase of  $1^{\circ}C$ , based on  
220 the seasonal global mean July surface air temperature range difference between model data  
221 of stadial conditions during MIS3 and the LGM. We calculated the differences in  $Wm^{-2}$  per  
222 month for each pair of consecutive reference dates and divided it by 4 to estimate the  
223 differences in  $^{\circ}C$ . We then added the difference per month to each day within that month.  
224 This of course leads to a slight overestimate of the early days and a slight underestimate of  
225 the late days in a month for the first half of the year and vice versa for the second half.

226 However, given the scope of this study, we consider the differences negligible.  
227 In doing so, we can estimate the start, end, length, and summed temperature of the growing  
228 season for each insolation reference date.

229  
230 The following results are shown for single time slices, as the difference between two  
231 consecutive time slices and as an accumulated trend over all time slices. By comparing  
232 changes in the spatial distribution of Core Areas between two time slices, possibly relating to  
233 expansions or contractions of human occupation, with changes in insolation, we analyse the  
234 impact of these changes on hunter-gatherer populations.

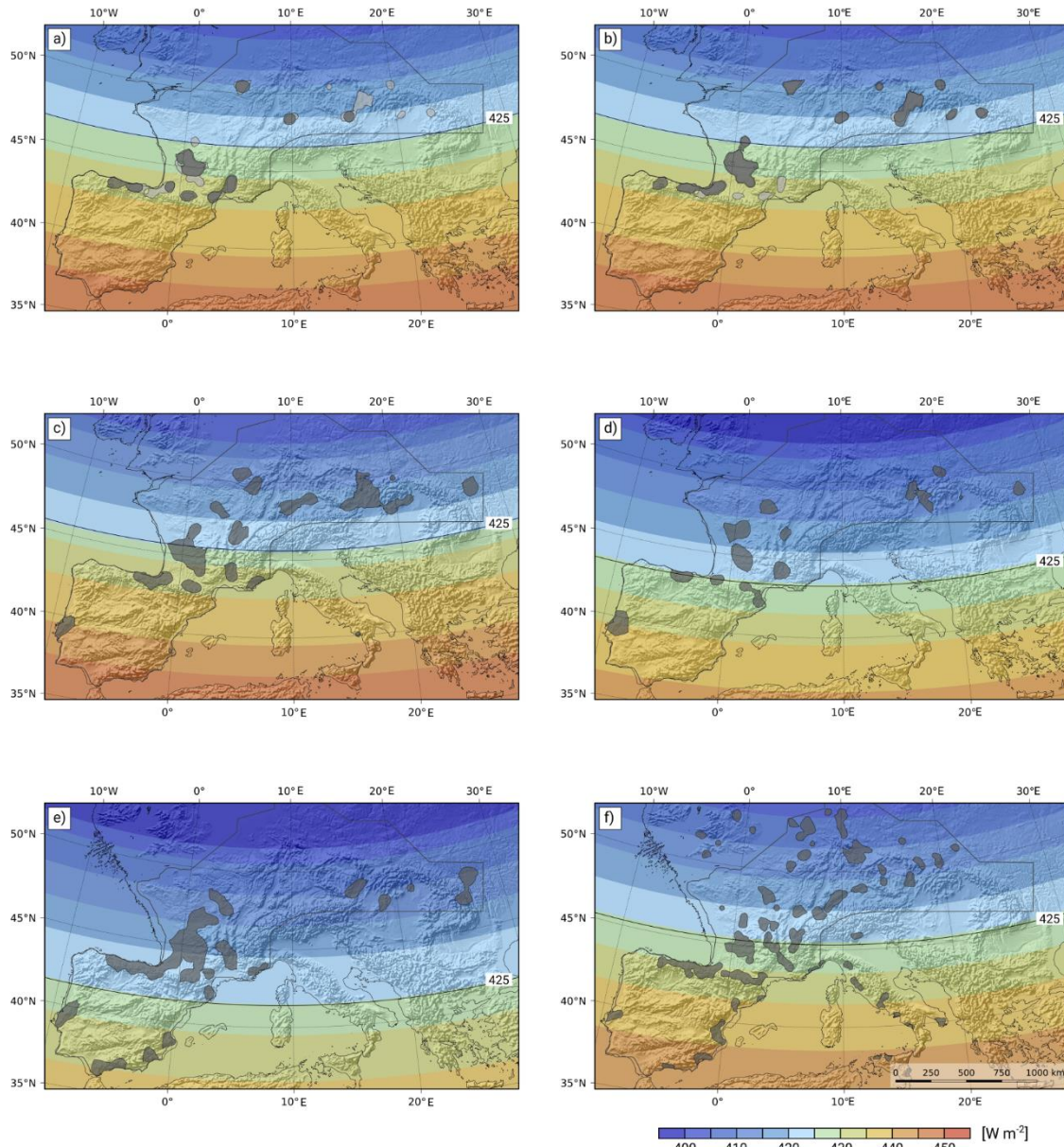
235  
236  
237  
238  
239  
240  
241  
242  
243  
244  
245  
246  
247  
248  
249

250  
251

**Table 1: Overview of timeframe and database for each phase.**

Archaeological Period	ka cal BP	Duration (ka)	Number of sites included	Number of sites / ky	Core Areas (km <sup>2</sup> )	Population size			Population density estimate per 2.3 Mio km <sup>2</sup>		
						min	median	max	min	median	max
Aurignacian (all)	42 - 33	9	382	43	<b>103,686</b>	<b>880</b>	<b>1,550</b>	<b>3,800</b>	0.038	0.067	0.165
<i>Aur P1 (Proto/Early)</i>	<i>n.a.</i>	5	117	23	<b>81,900</b>	<i>n.a.</i>	<i>n.a.</i>	<i>n.a.</i>	<i>n.a.</i>	<i>n.a.</i>	<i>n.a.</i>
<i>Aur P2</i>	<i>n.a.</i>	4	317	79	<b>128,600</b>	<i>n.a.</i>	<i>n.a.</i>	<i>n.a.</i>	<i>n.a.</i>	<i>n.a.</i>	<i>n.a.</i>
Gravettian P1	33 - 29	4	347	87	<b>243,039</b>	<b>1,660</b>	<b>2,760</b>	<b>3,610</b>	0.072	0.120	0.157
Gravettian P2	29 - 25	4	163	41	<b>123,810</b>	<b>660</b>	<b>1,000</b>	<b>1,530</b>	0.029	0.044	0.067
Last Glacial Maximum	25 - 20	5	396	79	<b>275,413</b>	<b>1,330</b>	<b>3,240</b>	<b>6,260</b>	0.058	0.141	0.272
Magdalenian (final)	20 - 15	5	1,002	200	<b>332,949</b>	<b>4,820</b>	<b>7,600</b>	<b>10,520</b>	0.210	0.33	0.46





252  
 253 **Figure 2: Distribution of Core Areas of the Upper Paleolithic plotted against insolation ( $Wm^{-2}$ ) during**  
 254 **growing season.** For reasons of comparability, the growing season is set from April to September in this graph.  
 255 Individual growing seasons are given in Figure 7 and Table 4. Latitudinal changes in insolation are highlighted by  
 256 the 425 in  $Wm^{-2}$  isoline for visualisation. Core Areas falling within the Total Area of Calculation (TAC, grey line)  
 257 are considered during further analysis. a) and b): 42-33 ka cal BP (Aurignacian P1 (a) and P2 (b) plotted in dark grey  
 258 onto *Aurignacian* all Core Areas in light grey), insolation at 37.5; c) 33-29 ka (Gravettian P1), insolation at 31  
 259 ka; d) 29-25 ka (Gravettian P2) insolation at 27 ka; e) 25-20 ka (LGM), insolation at 23.5 ka; f) 20-15 ka  
 260 (Magdalenian *final*), insolation at 17 ka. Coastline is -75 m b.c.s.l (a and b), -80 m b.c.s.l. (c and d), -120 m b.c.s.l.  
 261 (e) and -115 m b.c.s.l. (f) (taken from: Zickel et al. 2016).

262  
 263

### 264 3. RESULTS ON POPULATIONS SIZES, DISTRIBUTION AND INSOLATION

#### 265 3.1 PALEODEMOGRAPHIC ESTIMATES

266 The paleodemographic estimates (**Figure 1**) show an increase in the number of people  
 267 during the period from 42 to 33 ka (Aurignacian) and to the period between 33 and 29 ka  
 268 (Early Gravettian). This population growth is followed by a strong decline during the period  
 269 between 29 and 25 ka (Late Gravettian), with absolute numbers decreasing even below the  
 270 initial "starting" population at 42 ka. This decline coincides with a withdrawal from the higher  
 271 latitudes. The period between 25 and 20 ka (Solutrean, Badegoulian, Epigravettian) is a  
 272 period of population consolidation and renewed growth in Western Europe, while the  
 273

274 population in Central Europe remains at low levels. This only changed between 20 and 15  
 275 ka, when populations in both Western and Central Europe increased strongly and the higher  
 276 latitudes were resettled (**Table 1**).

277 In calculating the amount of overlap and discontinuity between the expanding, contracting,  
 278 newly emerging and vanishing Core Areas of consecutive time slices, it is possible to  
 279 quantify the spatial population dynamics. Here, overlapping Core Areas are seen as  
 280 indicative of continuity in human presence, whereas expanding or contracting ones are  
 281 understood as indicating discontinuity. Interestingly, percentages of areas either contracting  
 282 or expanding vary considerably through time, while spatial overlap of Core Areas for two  
 283 consecutive phases is constant and covers around 30% (**Table 2**) of the entire summed area  
 284 - except for the Magdalenian, where the rapid expansion of humans into northern latitudes  
 285 and the missing data for eastern Central-European sites produces a different pattern with a  
 286 reduced percentage of overlap. Generally, the percentage of overlapping Core Areas is  
 287 surprisingly low, given the constant presence of hunter-gatherers in Western Europe and  
 288 their quasi-constant presence in Central Europe (**Table 2**).

291 **Table 2: Percentages of overlapping, expanding and contracting Core Area sizes for**  
 292 **paired phases.**  
 293

Comparison of two Phases	Map in Figure B	Sum of Core Areas of two phases (sq km)	% Overlapping areas	% Expanded areas	% Contracted areas
Aurignacian P 1 and P2	(a)	157,750	33	48	18
<i>Aurignacian (all) and Grav. P1</i>	(b)	257,875	34	60	6
<i>Gravettian P1 and P2</i>	(c)	272,069	35	11	54
<i>Gravettian P2 and LGM</i>	(d)	310,713	28	60	11
LGM and Magdalenian	(e)	494,062	26	38	36

294  
 295  
 296 Note that the percentage of overlapping areas is quite constant through time, with decreases towards the  
 297 Magdalenian due to the overall expansion into northern latitudes.  
 298  
 299  
 300

**Table 3: Quantification of diachronic changes in Core Area sizes.**

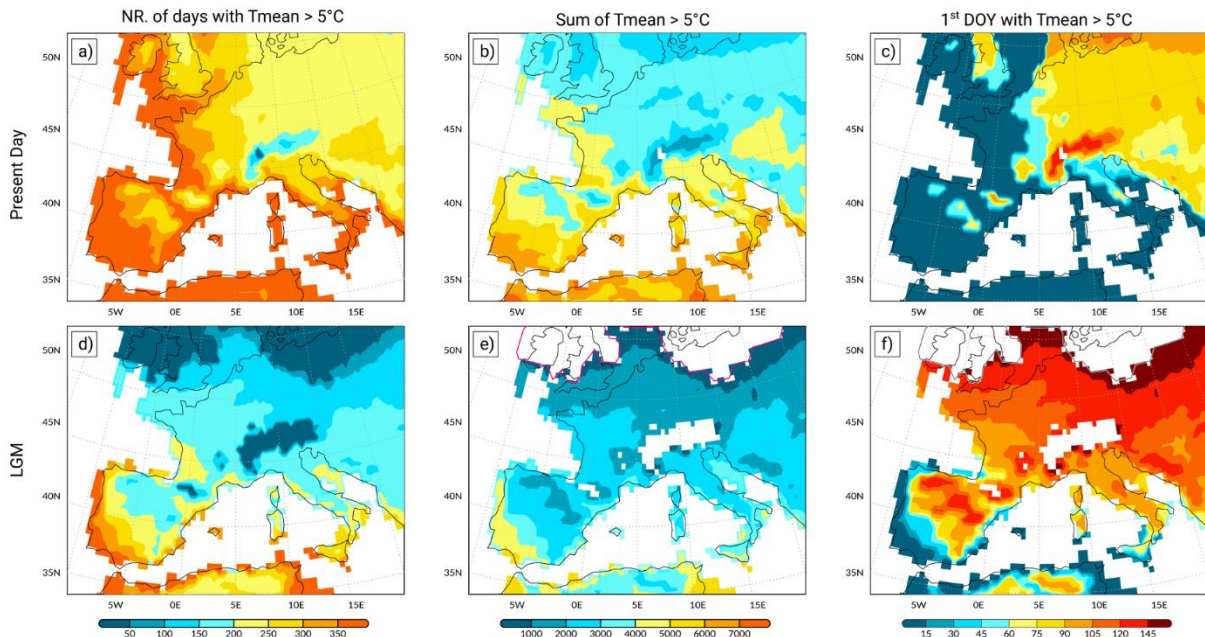
Phase	Core Areas (km <sup>2</sup> )	Continuity Discontinuities			Percentage of areas within a single phase			
		overlapping areas	expansion in comparison to previous phase	contraction in comparison to subsequent phase	overlapping in comparison to previous phase	expansion in comparison to previous phase	Sum	contraction in comparison to subsequent phase
		(km <sup>2</sup> )	(km <sup>2</sup> )	(km <sup>2</sup> )	%	%	%	%
Aurignacian	103,686	n.a.	n.a.	14,836	n.a.	n.a.	n.a.	14
<i>Aur P1 (Proto/Early)</i>	81,900	n.a.	n.a.	29,150	n.a.	n.a.	n.a.	36
<i>Aur P2 (Late)</i>	128,600	52,750	75,850	n.a.	41	59	100	n.a.
Gravettian P1	<b>243,039</b>	88,850	154,189	148,259	37	63	100	61
Gravettian P2	<b>123,810</b>	94,780	29,030	35,300	77	23	100	29
Last Glacial Maximum	<b>275,413</b>	88,510	186,903	161,113	32	68	100	58
Magdalenian	<b>332,949</b>	114,300	218,649	n.a.	40	60	100	n.a.

301 Size and percentage of overlapping, contracting and expanding Core Areas are compared for each phase to  
 302 previous (areas of overlap and expansion) and subsequent phases (areas of contraction).  
 303  
 304  
 305



306 3.2 INSOLATION AND GROWING SEASON

307 An overview of the length, summed temperature and start of the growing season based on  
 308 the regional climate model data for LGM and present day is given in **Figure 3** and **Table 4**.  
 309 The number of days with daily mean temperature above 5°C are obviously much lower for  
 310 LGM climate conditions, which is in accordance to a much lower summed temperature during  
 311 the growing season for LGM conditions. Likewise, there is a pronounced shift of the 1<sup>st</sup> day of  
 312 the year when daily mean temperatures above 5°C were simulated. For present day climate,  
 313 large parts of Western Europe already reach the first day with mean daily temperature above  
 314 5°C already in January. For LGM climate conditions, there is a shift of ~3 months into the  
 315 year until mean daily temperatures reach values above 5°C.  
 316  
 317



318 **Figure 3: Parameters relevant for the growing season based on WRF model output for present day**  
 319 **climate:** (a) number of days with a mean daily temperature > 5°C; (b) temperature sum of all days within the  
 320 growing season and (c) the first day of the year with a mean daily temperature > 5°C. (d)-(f) same as (a)-(c) but  
 321 for LGM climate conditions.  
 322  
 323

324 When looking at the changes in MJm<sup>-2</sup> for each month through the succession of the insolation reference dates as  
 325 differences between consecutive reference dates (**Figure 4**), it becomes clear that the strongest differences  
 326 throughout the period of observation occur during the months from April to October with differences of up to 60  
 327 MJm<sup>-2</sup> in May and June, while the insolation from December to February remained rather stable.  
 328

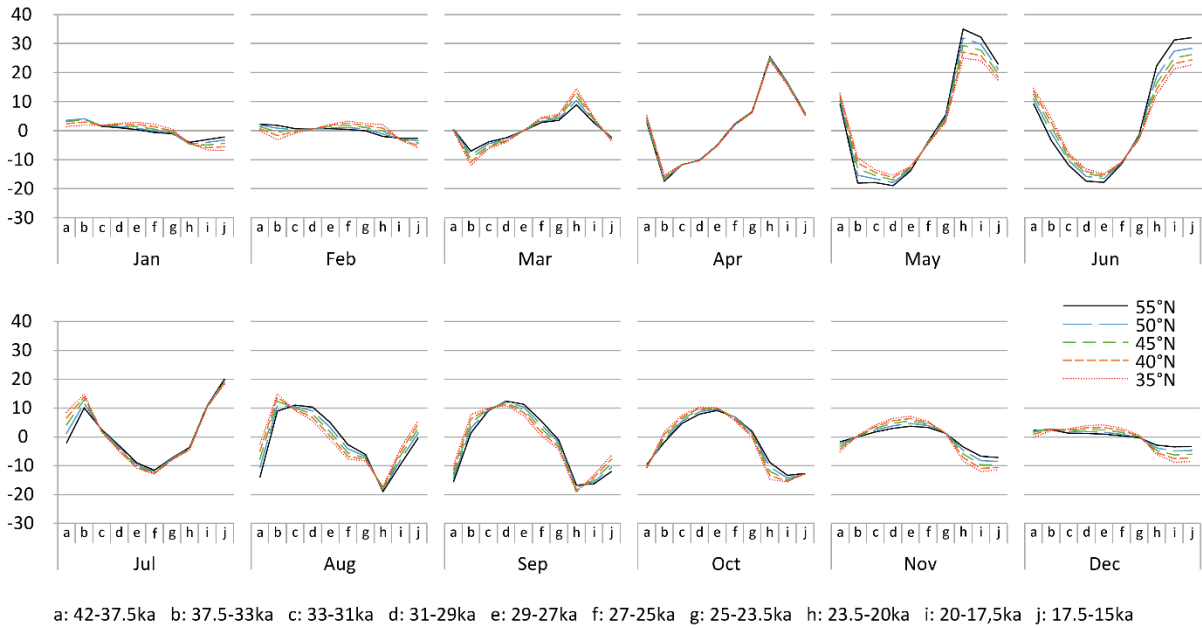
329 The accumulated differences throughout the entire period of observation (**Figure 5**) show  
 330 that highest losses in solar energy occur during the month of May and June between 29 and  
 331 25 ka, whereas the highest gains can be observed for September and October of the same  
 332 period.  
 333

334 **Figure 6** shows changes in MJm<sup>-2</sup> throughout the year as differences between two  
 335 consecutive insolation reference dates. After an initial gain in insolation in the first part of the  
 336 year and a loss in the second from 42 to 37.5 ka, each of the following four units (37.5 to 27  
 337 ka) show the opposite trend with losses in the first half and gains in the second half. From 27  
 338 to 25 ka, the loss shifts to the middle of the year, while both the early and late parts of the  
 339 year gaining energy. From 23.5 ka onwards, the system shifts back to the first pattern, with  
 340 gains during the first half and losses during the second, but with a much higher amplitude. At  
 341 15 ka, a shift of energy gain towards the middle of the year is again observable.  
 342

343 Considering the accumulated differences with regard to the position and length of the  
 344 growing season at 45°N (**Figure 7, 8, Table 4**) is very informative and reveals long-term

345 changes. Three things are particularly remarkable. First, the shift from a gain of insolation  
 346 during the first half to a pronounced loss and back to a strong gain with a complementary  
 347 development during the second half becomes much clearer. Second, more or less in  
 348 accordance with this shift, is a delay in the start of the growing season from mid-April  
 349 between 42 and 37.5 ka to mid-May between 27 and 25 ka. The end of the growing season  
 350 also shifts backwards. Third, is the particularly conspicuous loss of solar energy during the  
 351 start of the growing season between 29 and 21 ka. Between 27 and 25.5 ka, plants have  
 352 about 60 MJm<sup>-2</sup> less for their photosynthesis during the crucial early part of the growing  
 353 season.

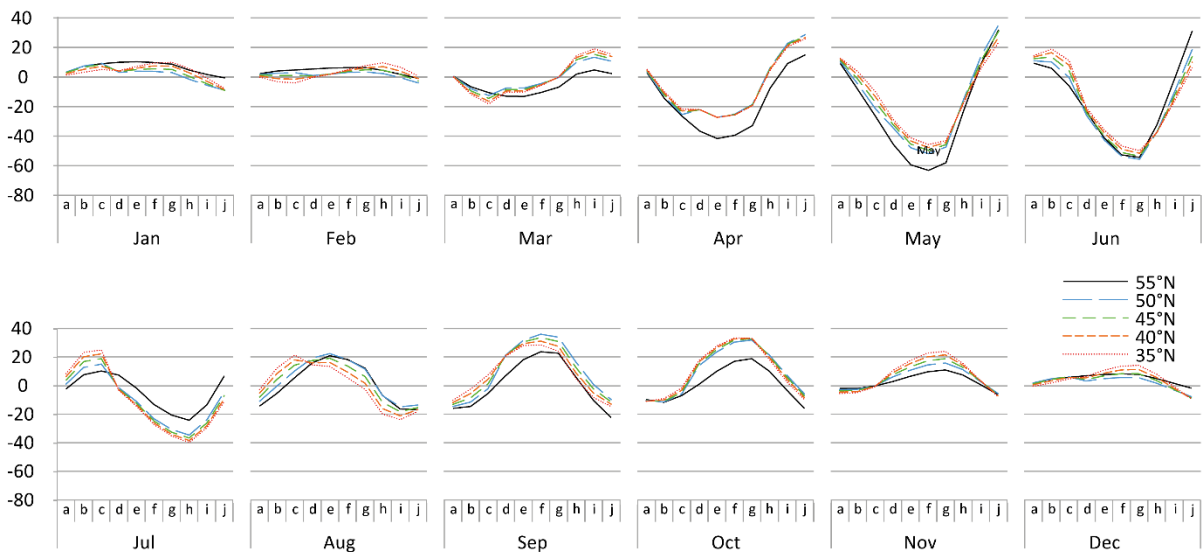
354  
355



356  
357  
358  
359  
360

a: 42-37.5ka b: 37.5-33ka c: 33-31ka d: 31-29ka e: 29-27ka f: 27-25ka g: 25-23.5ka h: 23.5-20ka i: 20-17.5ka j: 17.5-15ka

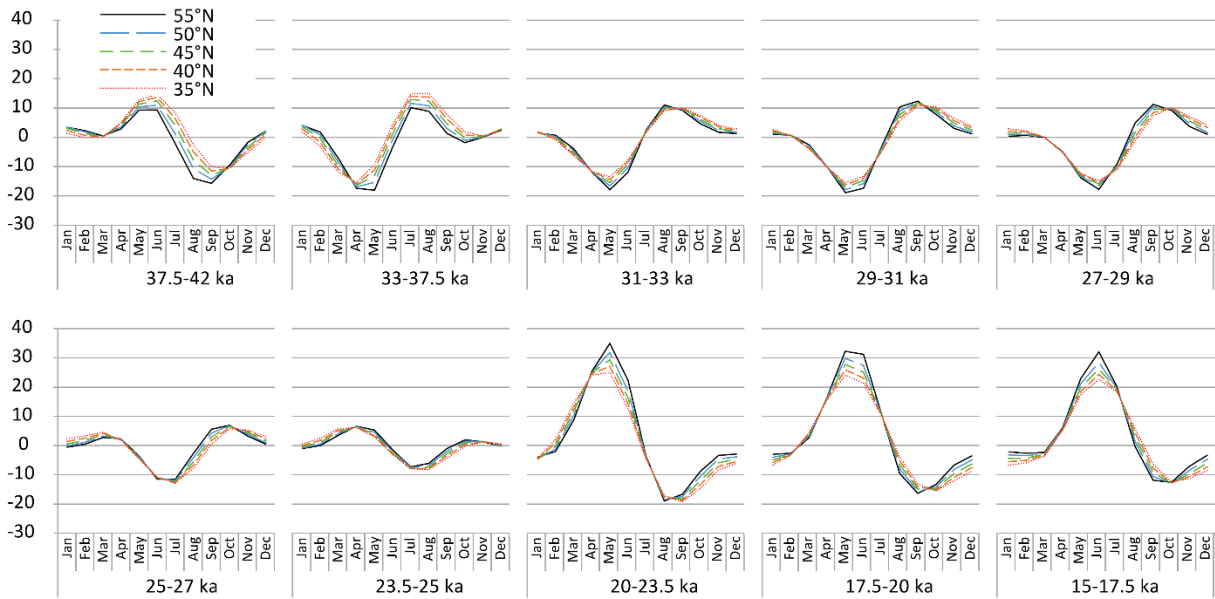
**Figure 4:** Differences in MJm<sup>-2</sup> for each month through the succession of the insolation reference dates as differences between two consecutive reference dates.



361  
362  
363  
364

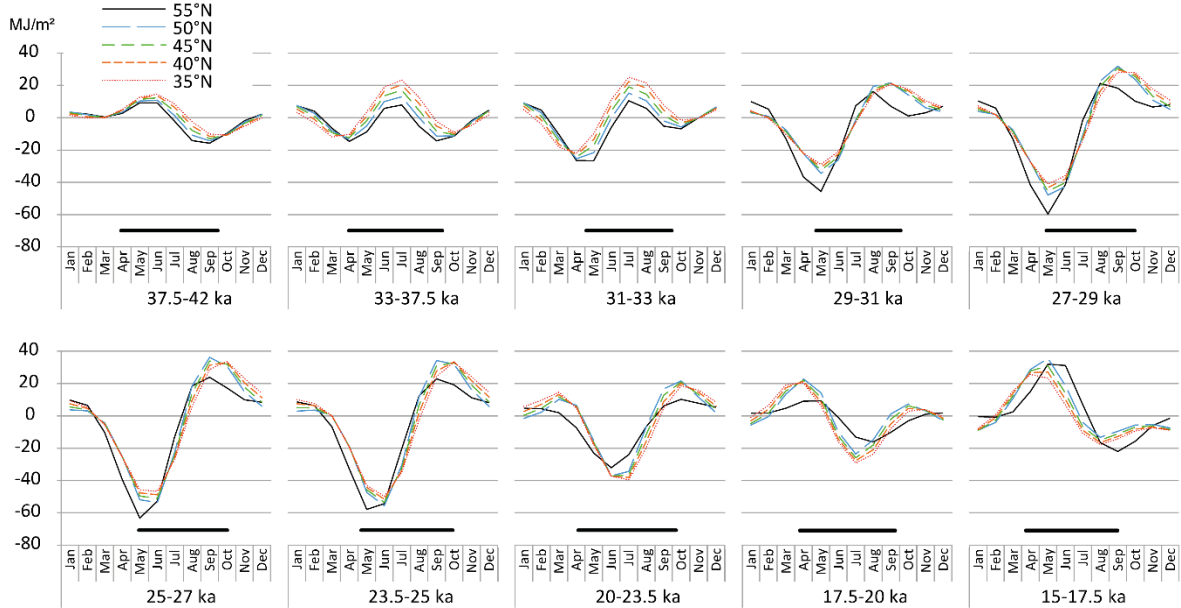
a: 42-37.5ka b: 37.5-33ka c: 33-31ka d: 31-29ka e: 29-27ka f: 27-25ka g: 25-23.5ka h: 23.5-20ka i: 20-17.5ka j: 17.5-15ka

**Figure 5:** Differences in MJm<sup>-2</sup> for each month through the succession of the insolation reference dates as accumulated differences throughout all reference dates. For legend see Figure 4.



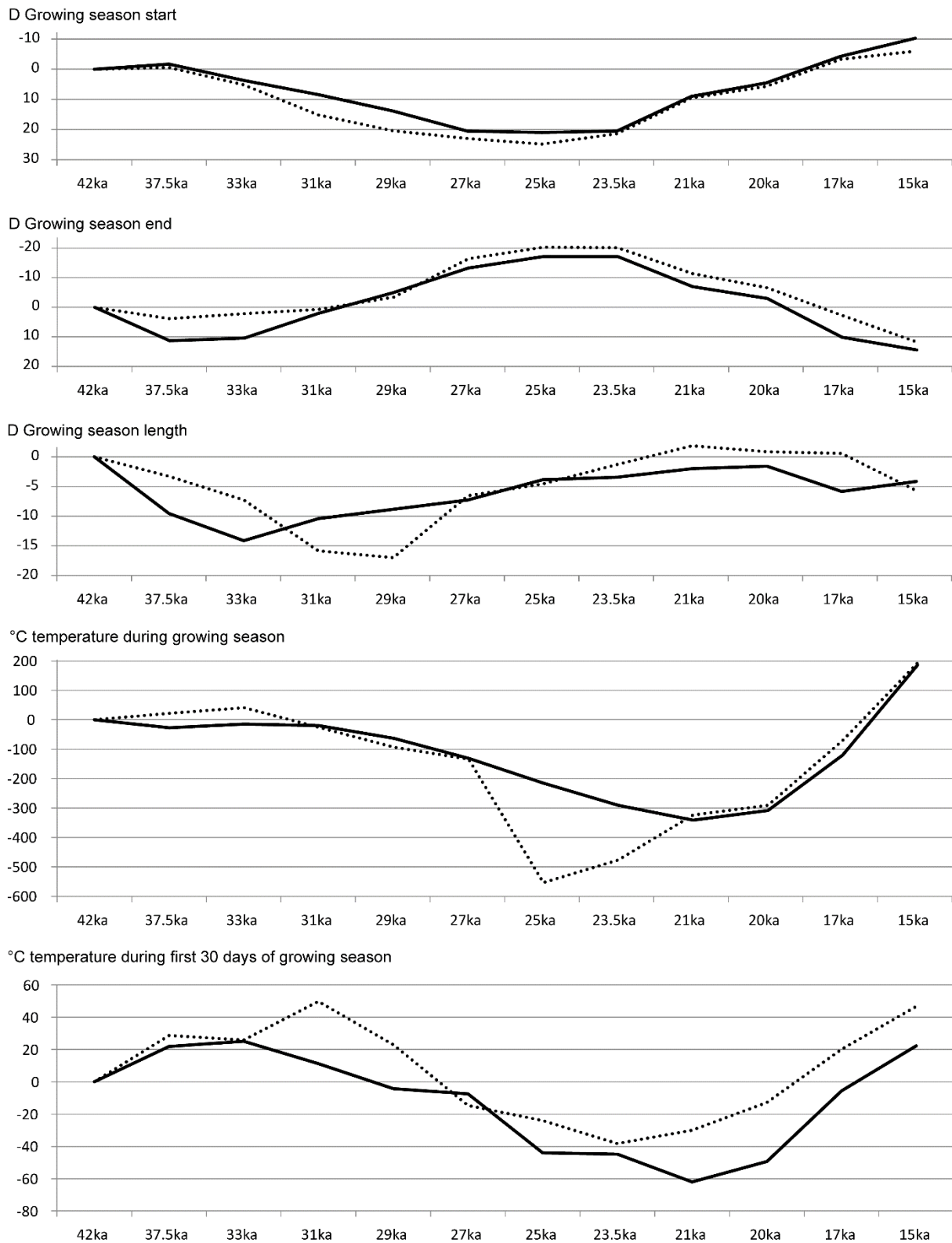
365  
366  
367  
368  
369  
370

**Figure 6.** Changes in  $\text{MJm}^{-2}$  throughout the year as differences between two consecutive insolation reference dates. For legend see Figure 4.



371  
372  
373  
374  
375

**Figure 7.** Changes in  $\text{MJm}^{-2}$  throughout the year as accumulated differences between consecutive insolation reference dates. Solid bars indicate position and length of the growing season at  $45^{\circ}\text{N}$  (see **Table 4**). For legend see Figure 4.



376  
 377  
 378  
 379  
 380  
 381  
 382  
 383  
 384  
 385

**Figure 8.** Changes in start, end, length, summed temperatures and summed temperatures during the first 30 days of the growing season at 45°N (dotted line) and 50°N (solid line).

386  
387

**Table 4. Parameters of the growing season.**

		42ka	37.5ka	33ka	31ka	29ka	27ka	25ka	23.5ka	21ka	20ka	17ka	15ka
50°N	$\Sigma T$ in °C*	1,77 2	1,74 5	1,75 7	1,75 3	1,71 0	1,64 1	1,55 7	1,48 1	1,43 1	1,46 4	1,65 2	1,95 8
	Start in calendar day*	127	125	131	135	141	148	148	148	136	132	123	117
	End in calendar day*	261	250	251	259	266	275	279	279	268	264	251	247
	Length in calendar days*	135	126	121	125	127	128	132	132	133	134	130	131
45°N	$\Sigma T$ in °C*	2,57 2	2,59 4	2,61 3	2,54 6	2,47 9	2,43 8	2,01 8	2,09 5	2,24 8	2,28 2	2,50 2	2,76 6
	Start in calendar day*	169	166	162	153	152	163	165	168	171	170	170	163
	End in calendar day*	107	106	112	122	127	130	132	128	116	113	104	101
	Length in calendar days*	275	271	273	274	278	291	295	295	286	282	272	263
	$\Sigma T$ in C° of first 30 days	291	320	317	341	314	277	267	253	261	279	312	338

388  
389  
390

All values represent averages from 7 longitudes at -1°, 3.5°, 8°, 12.5°, 17°, 21.5°, and 26° E.

391  
392  
393  
394

#### 4. DISCUSSION

395  
396

##### 4.1 A DIACHRONIC COMPARISON OF POPULATION DYNAMICS AND CHANGES IN SOLAR INSOLATION

397  
398  
399  
400

In order to assess the possible impact of changes in insolation on the demographic developments of the Upper Palaeolithic in Europe, we compare the results of both analyses diachronically. Here, shifts in Core Areas are taken as indicators for spatial population dynamics.

401  
402

##### 4.1.1 42-33 ka – Aurignacian

403  
404  
405  
406  
407  
408  
409  
410  
411  
412  
413  
414  
415  
416

For this period connected with the first extensive spread of anatomically modern humans into Central and Western Europe, we estimate a mean population size of 1,500 persons (max.1,800 / min. 700; Schmidt and Zimmermann 2019). Core Areas were calculated for an early phase (Proto and Early Aurignacian; Aur P1) and later phases (Aur P2; **Figure 2: a, b**), although paleodemographic estimates for these two sub-phases were not possible and are therefore given for the entire Aurignacian (Aurignacian *all*, see **Table 1**) (ibid.). It becomes clear that both phases show regional differences in their spatial pattern and several indicators (e.g. number of sites per 1,000 years, size of the Core Areas) support a population increase from the early to the late phase, particularly in the eastern part of the investigated area. Continuity through both phases can be attested for regions where viable populations have been estimated for the entire Aurignacian (ibid.: **Figure 2** and **Table 3**). However, almost 60 % of the area covered during the later phase relates to newly emerging and expanding Core Areas (**Table 3**), occurring mainly in Northern Iberia, SW-France and the Middle Danube/Moravian Region (**Figure 9: a**).

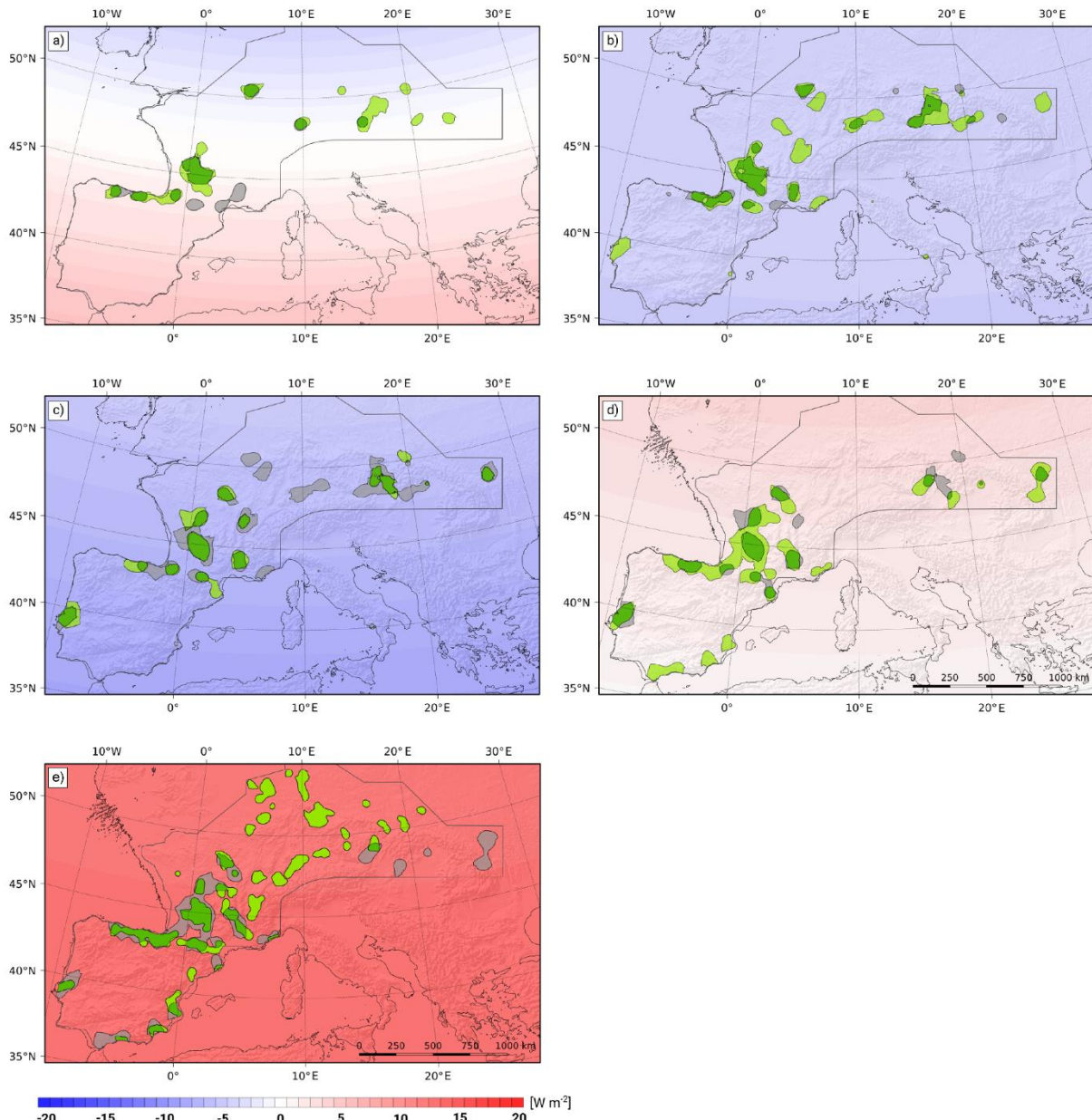
417  
418  
419  
420  
421  
422  
423  
424

With regard to the environmental data, we observe some changes. While there is a slight trend towards a later start and shortening of the growing season (**Figure 8**), the summed temperature during the entire growing season and during the first 30 days are both rising with a first peak of the latter at 37.5 ka and of the former at 33 ka (**Table 4**). This gain seems to be more pronounced in Central than in Western Europe. Between 42 and 37.5 we see a rise in solar energy during the early growing season followed by a shift of maximum insolation to the middle part of the year between 37.5 and 33 ka (**Figure 7**).



425 4.1.2 33-29 ka – Early Gravettian

426 The demographic trend continues during the first half of the Gravettian and the overall  
 427 estimate of people rises to a median of 2,800 (+900 / -1,100; Maier and Zimmermann 2017).  
 428 Core Areas with viable populations during the Aurignacian expand, especially in the Upper  
 429 and Middle Danube/Moravian Regions and new ones emerge across the entire TAC,  
 430 extending to the East and Southwest of Europe (**Figure 9: b**). Again, the areal increase  
 431 ranges around 60%, with an exceptionally low “loss” of regions covered by Core Areas  
 432 during the Aurignacian (only 14%). Estimated population density within the Core Areas,  
 433 however, varies considerably from 2.7 to 0.3 persons per 100 km<sup>2</sup> (median often around 1.4,  
 434 ibid).  
 435



436  
 437  
 438 **Figure 9: Diachronic changes of Insolation and Core Areas during the Upper Palaeolithic.** Core Areas are  
 439 displayed for two successive periods. Colours indicating continuity (dark green), expansion (light green) and  
 440 contraction (grey areas) of Core Areas. Changes in insolation (W/m<sup>2</sup>, see legend) during the respective phases  
 441 are given as the difference between insolation at the end of each phase. a) Difference of insolation between 37.5  
 442 and 33 ka (Aurignacian P1 and P2); b) between 33 and 29 ka (Aurignacian all and Gravettian P1); c) between 29  
 443 and 25 ka (Gravettian P1 and P2); d) between 25 and 20 ka (Gravettian P2 and LGM); e) between 20 and 15 ka  
 444 (LGM and Magdalenian). For reconstructed coastlines and TAC see **Figure 2**.  
 445



446 A look at the environmental data shows that this phase is characterised by a continuation of  
447 the moderate decline during the first half of the year, coinciding with a slight delay in the  
448 onset of the growing season in comparison to previous periods (**Figure 7** and **8**). This trend  
449 is counteracted, however, by a strong gain in temperatures during the first 30 days of the  
450 growing season with the highest values of the entire period of observation at 31 ka (**Figure**  
451 **8**).

#### 452 453 4.1.3 29-25 ka Late Gravettian

454 The most exceptional and marked decrease in population size and distribution during the  
455 entire Upper Palaeolithic of Europe has been detected for the later phase of the Gravettian  
456 (**Figure 9: c**), with estimates dropping to a median value of 1,000 (+500 / -300; Maier and  
457 Zimmermann 2017). Core Areas disappear in Western Central Europe and experience  
458 considerable contraction and fragmentation in all other regions of Europe, except for central  
459 Portugal. In comparison with the first half of the Gravettian, the spatial loss amounts to 61%  
460 (**Table 3**, see also **Table 2**). Only a few Late Gravettian Core Areas actually show evidence  
461 of an expansion (23%) and thus it is not surprising that the Core Areas of the Late Gravettian  
462 overlap – also to an exceptionally high percentage of 77% - within the areas already  
463 occupied previously.

464  
465 Interestingly, the strong demographic decline coincides with the maximum delay in the start  
466 of the growing season coupled with the maximum loss of solar energy during its early phase  
467 (**Figure 7**). At the same time, the sum of temperatures during the growing season drops  
468 sharply towards 25 ka to the lowest values in the entire period of observation (**Figure 8**). The  
469 renewed prolongation of the length of the growing season back to the level of 33 ka  
470 apparently does not counteract these effects. In this context it is interesting to note the cave  
471 bear, a species that was apparently reliant on high-quality plant food which made it  
472 vulnerable to decreasing vegetational productivity, goes extinct in Central Europe at around  
473 28 ka (Pacher and Stuart 2008).

#### 474 475 4.1.4 25-20 ka – The Last Glacial Maximum – Solutrean, Badegoulian, Early Epigravettian

476 During the Last Glacial Maximum, we see a turnaround in the demographic downward trend.  
477 Mean population estimates of 3,100 (+3,200 / - 1,800) show renewed population growth  
478 (Maier et al. 2016). However, it is only in Western Europe that this growth is apparent,  
479 whereas populations in Central Europe remain at a low level. Furthermore, increasing the  
480 temporal resolution within this period of 5 ka, it seems that roughly between 22 and 21 ka,  
481 there is no evidence of hunter-gatherer north of 47°N. Previous tendencies towards  
482 fragmentation of Core Areas disappear in southwestern / northern Iberia and turn into  
483 expansion and even merging of Core areas (**Figure 9: d**). In southern Iberia, the Cologne  
484 Protocol detects Core Areas along the Mediterranean coast for the first time.

485 Environmentally, we again see an increasingly early start of the growing season, and the  
486 growing season length even peaks at 21ka. After a minimum at 23.5 ka, the summed  
487 temperatures of the first 30 days of the growing season rise again as does the sum of  
488 temperature during the entire growing season. In addition, we see a slight increase in solar  
489 energy during the first half of the year between 25 and 23.5 ka becoming a bit more  
490 pronounced between 23.5 and 20 ka. However, Verpoorte (2009) notes a marked decline in  
491 the diversity of the faunal assemblages of Central Europe occurring at around 24 ka. A  
492 similar pattern is reported by Jochim (1987) for south-western France. This might be related  
493 to a delay in the faunal response because of a certain inertia of population dynamics with  
494 regard to change in the environmental system.

#### 495 496 4.1.5 20-15 ka – Magdalenian

497 Between 20 and 15 ka, the estimated number of people rises markedly to a mean of 7,700  
498 (+3,000 / - 2,800), while the density in Core Areas ranges between 1.6 and 3.6 persons per  
499 100 km<sup>2</sup> (Kretschmer 2015). With regard to spatial dynamics, it has to be stated that Core  
500 Areas are only available for Western Europe and the western part of Central Europe, since  
501 Epigravettian sites, located further East, have not been considered in the estimates. This

502 does, to some extent, explain the relatively high percentages (58%) of contracting areas  
503 compared to the period of the LGM given in **Table 3**. Other contractions can be observed in  
504 south-western Europe (**Figure 9: e**). However, the general trend of continuity (40%) and  
505 expansion (60%) in the spatial distribution of final Magdalenian Core Areas already observed  
506 during the LGM does continue: together with the increasing population and the resettlement  
507 of the higher latitudes, we see an increasingly early start of the growing season (the earliest  
508 of the entire study at 15 ka) coupled with increasing summed temperatures for both the entire  
509 growing season (highest in the entire study at 15ka) and the first 30 days (second highest  
510 after 31 ka; **Figure 8**). In addition, there is a strong increase in solar energy during the first  
511 half of the year and thus also during the beginning of the growing season (**Figure 7**).

512  
513

#### 514 4.2 INSOLATION AS A PACEMAKER FOR LONG-TERM DEMOGRAPHIC 515 DEVELOPMENTS?

516 For Palaeolithic hunter-gatherers, who extracted all their energy directly from their  
517 environment without further manipulation, the availability and diversity of animal biomass is  
518 probably a key-factor allowing their continued presence in a region (Tallavaara et al. 2018).  
519 For Western and Central Europe, terrestrial herbivores were the most important game. In  
520 addition to their role in human nutrition, they also provided useful raw materials, such as  
521 antler, bone or ivory, making them crucial in the entire subsistence system (Soulie et al. 2014;  
522 Soulie et al. 2014). The abundance and diversity of herbivores in a landscape depends  
523 essentially on the availability and quality of plant food in a region (Olff et al. 2002).

524 Usually when thinking about availability of (plant) food, quantity and quality are the factors  
525 being considered. However, timing also seems to be of major importance. After long glacial  
526 winters, herbivorous animals depend on the availability of sufficient high-quality plant food in  
527 spring. Not only do they have to replenish their reserves, but this is also the period when  
528 their offspring are born. Spring is thus a crucial period for herbivorous animals and one  
529 during which they are rather vulnerable to shifts in plant phenology and environmental stress  
530 (Debeffe et al. 2019). The green-up of the landscape is also a key-factor for the timing and  
531 movements of ungulates for spring migration (Merkle 2016). Shifts, delays, and unforeseen  
532 changes in the migration patterns of their most important prey species, in turn, have a high  
533 potential to cause problems for hunter-gatherers (Krupnik 2018; Mandryke 1993; Smith  
534 1978). As shown above, spring is the period affected the most by the changes in solar  
535 insolation between 43 and 15 ka. Between 25 and 23.5 ka, the growing season was delayed  
536 by about a month. Moreover, when it started, the available solar energy and temperatures  
537 were very low. Low temperatures also have negative influence on seed germination and  
538 seedling establishment (Trugdill et al. 2000; Zhang et al. 2018). The cooling effect of  
539 permafrost on soil temperature likely further hampered germination at 25ka, impeding the  
540 start of the growing season and thus biomass production even more strongly than estimated  
541 from insolation alone. Additionally, a lower CO<sub>2</sub> level (Van Meerbeeck et al. 2009) probably  
542 reduced the growth of at least C3-plants (Bartlein et al. 2010) and waterlogging in the active  
543 layer of permafrost soils likely further handicapped plant growth. Impeded germination  
544 eventually leads to fewer mature plants and less seeds for the following year, leading to a  
545 self-reinforcing reduction of the vegetation. It can thus be surmised that between 25 and 23.5  
546 ka plant food was available only considerably later during the year, and when it appeared,  
547 overall biomass production was rather low. This likely caused substantial problems and  
548 environmental stress for herbivorous populations, especially in higher latitudes (Belovsky  
549 1988; Mandryk 1993: 56). Such a shift in seasonality with a prolongation of the winter-period  
550 and a severely delayed start of the growing season might also explain the peculiar finding of  
551 virtual absence of mammoth during the LGM in large parts of Europe (Stuart 2005). With  
552 their high demand for plant food, the carrying capacity during springtime may have been too  
553 low to support a viable mammoth population.

554 The changes in solar insolation and the dependent vegetational system probably led to a  
555 loss of animal diversity, delayed spring migrations and eventually a strong reduction and/or

556 withdrawal of larger herbivores from higher latitudes. In combination, these factors probably  
557 made the northern areas also inhospitable for hunter-gatherers, who apparently vanished  
558 from these regions. However, the lower latitudes were also affected by decreasing spring  
559 insolation with presumably negative effects on the net production of primary biomass; this is  
560 congruent with a general population decline at around 25 ka in Western and Central Europe.  
561 It is only with a renewed increase in spring insolation and an ever-earlier start to the growing  
562 season after 20ka, that populations in Western and Central Europe showed a considerable  
563 increase in numbers and densities and an expansion of their Core Areas into the higher  
564 latitudes.

565 Ultimately, it can be stated that this parallel development in palaeodemography and solar  
566 insolation is unlikely to be merely coincidental. It seems that for the spatially large-scale and  
567 long-term development of hunter-gatherer populations, in terms of both their numbers and  
568 distribution, solar insolation is an important driver.

569

570

## 5. CONCLUSION

571 It seems that ecosystems in Europe between 43 and 15 ka reacted very sensitively to gains  
572 and losses in solar energy and potentially resulting changes in plant and animal phenology.  
573 This effect seems to be particularly pronounced in the higher latitudes (cf. Feurdean et al.  
574 2014), but affected the lower ones as well. Stronger reactions in the north are likely a  
575 consequence of generally lower temperatures and insolation values. Hence, while a  
576 reduction in the lower latitudes still left enough energy for a timely start of the growing  
577 season, a reduction at higher latitudes may have quite noticeable and rather severe  
578 consequences. For hunter-gatherers depending on the resources provided by their  
579 environment, it is not the total amount of annual insolation that is important. Rather it is the  
580 available energy during the growing season that, via plant biomass and herbivorous animals,  
581 affects the basis of existence of Palaeolithic hunter-gatherers. Interestingly, a late onset of  
582 the growing season seems to have more severe consequences for the ecosystem than a  
583 shorter duration.

584 Anatomically modern humans arrived in Europe during a period of medium intensity solar  
585 insolation. Subsequently, a moderate gain in insolation during the growing season was  
586 accompanied by moderate population growth and spatial extension of the Core Areas. Over  
587 the following millennia, the coupled effects of a late start to the growing season, a reduced  
588 amount of energy during its early phase, and a low overall temperature throughout its  
589 duration likely led to a considerable reduction in plant biomass availability until around 23.5  
590 ka. It is highly likely that this development led to a reduction of the diversity and abundance  
591 of herbivorous animals in the landscape and might be part of the explanation for the virtual  
592 absence of mammoth during the LGM. We hence argue for assuming an indirect causal  
593 relationship, mediated by changes in animal abundance, between the decline of solar  
594 insolation and the pronounced decline of hunter-gatherer populations in Western and Central  
595 Europe between 29 and 25 ka. The same causal relationship can be assumed between the  
596 increase in spring insolation, an ever-earlier starting growing season and the demographic  
597 growth and spatial expansion of hunter-gatherer groups after 23.5 ka ago.

598

## 599 ACKNOWLEDGEMENTS

600 This publication was funded by the German Research Foundation – Project-ID 57444011 –  
601 SFB 806 “Our Way to Europe”. We thank two anonymous reviewers as well as Jayson Orton  
602 for his insightful comments on content and the English language, and Nina Avci for  
603 assistance during editing. All mistakes are our own.

604

605 **References**

- 606 Bartlein, P. J., Harrison, S. P., Brewer, S., Connor, S., Davis, B. A. S., Gajewski, K., Guiot, J., Harrison-  
607 Prentice, T. I., Henderson, A., Peyron, O., Prentice, I. C., Scholze, M., Seppä, H., Shuman, B., Sugita S.,  
608 Thompson, M. R. S., Viau, A. E., Williams, J., Wu, H., 2010. Pollen-based continental climate  
609 reconstructions at 6 and 21 ka: a global synthesis. *Climate Dynamics* 37, 775-802. DOI  
610 10.1007/s00382-010-0904-1.
- 611 Berger, A.L., 1978. Long-term variations of daily insolation and Quaternary climatic changes. *Journal*  
612 *of the Atmospheric Sciences* 35, 2362-2367.
- 613 Bocquet-Appel, J.-P., Demars P.-Y., 2000. Population Kinetics in the Upper Palaeolithic in Western  
614 Europe. *Journal of Archaeological Science* 27, 551-570.
- 615 Bocquet-Appel, JP., Demars, P., Noiret, L., Dobrowsky, D., 2005. Estimates of Upper Palaeolithic  
616 meta-population size in Europe from archaeological data. *Journal of Archaeological Science* 32,  
617 1656–1668.
- 618 Boserup, E., 1965. The conditions of agricultural growth. The economics of agrarian change under  
619 population pressure. UK: Allen & Unwin Ltd, London.
- 620 Both, C., Van Turnhout, C. A. M., Bijlsma, R. G., Siepel, H., Van Strien A. J., Foppen, R. P. B., 2010.  
621 Avian population consequences of climate change are most severe for long-distance migrants in  
622 seasonal habitats. *Proceedings of the Royal Society B: Biological Sciences* 277, 1259–1266.  
623 doi:10.1098/rspb.2009.1525.
- 624 Bradtmöller, M., Pastoors, A., Weniger, G.-C., 2010. The repeated replacement model - Rapid climate  
625 change and population dynamics in Late Pleistocene Europe. *Quaternary International* 247, 38-49.  
626 DOI: 10.1016/j.quaint.2010.10.015.
- 627 Braconnot, P., Harrison, S. P., Kageyama, M., Bartlein, P. J., Masson-Delmotte, V., Abe-Ouchi, A.,  
628 Otto-Bliesner, B., Zhao, Y., 2012. Evaluation of climate models using paleoclimatic data. *Nature*  
629 *Climate Change* 2, 417–424. DOI:10.1038/nclimate1456.
- 630 Burrows, M. T., Schoeman, D. S., Buckley, L. B., Moore, P., Poloczanska, E. S., Brander, K. M., Brown,  
631 C., Bruno, J. F., Duarte, C. M., Halpern, B. S., Holding, J., Kappel, C. V., Kiessling, W., O'Connor, M. I.,  
632 Pandolfi, J. M., Parmesan, C., Schwing, F. B., Sydeman, W. J., Richardson, A. J., 2011. The pace of  
633 shifting climate in marine and terrestrial ecosystems. *Science* 334, 652–655.  
634 doi:10.1126/science.1210288.
- 635 Crucifix, M., 2016. palinsol: Insolation for Palaeoclimate Studies. R package version 0.93.  
636 <https://CRAN.R-project.org/package=palinsol>.
- 637 Debeffe, L., Rivrud, I. M., Meisingset, E. L., Mysterud, A., 2019. Sex-specific differences in spring and  
638 autumn migration in a northern large herbivore. *Scientific Reports* 9.  
639 <https://doi.org/10.1038/s41598-019-42639-3>.
- 640 Demidenko, Y., 2018. Gravettian in the Great North Black Sea Region in the Context of East European  
641 Upper Palaeolithic. *Stratum Plus* 1, 265-283.
- 642 Feurdean A, Perşoiu A, Tanţău I, Stevens T, Markovic, Magyari EK, Onac BP, Andric M, Connor S, Galka  
643 M, Hoek WZ, Lamentowicz M, Sümegi P, Perşoiu I, Kolaczek P, Kunes P, Marinova E, Slowinski M,  
644 Michczynska D, Stancikaite M, Svensson A, Veski S, Fărcaş, Tămaş, Zernitskaya V, Timar A, Tonkov S,  
645 Toth M, Willis KJ, Plóciennik M, Gaudeny T(2014) Climate variability and associated vegetation  
646 response throughout Central and Eastern Europe (CEE) between 8 and 60 kyrs ago. *Quaternary*  
647 *Science Reviews* 106, 206–224.

- 648 French, J. C., 2015. Demography and the palaeolithic archaeological record. *Journal of Archaeological*  
649 *Method and Theory* 23, 150–199.
- 650 French, J. C., 2018. Archaeological demography as a tool for the study of women and gender in the  
651 past. *Cambridge Archaeological Journal* 29, 1–17.
- 652 French, J. C., Collins, C., 2015. Upper Palaeolithic population histories of Southwestern France: a  
653 comparison of the demographic signatures of 14C date distributions and archaeological site counts.  
654 *Journal of Archaeological Science* 55, 122-134.
- 655 Fu, Q., Posth, C., Hajdinjak, M., Petr, M., Mallick, S., Fernandes, D., et al., 2016. The genetic history of  
656 Ice Age Europe. *Nature* 534, 200–205.
- 657 Gamble, C. S., 2002. *The Palaeolithic Settlement of Europe*. Cambridge University Press, Cambridge.
- 658 Gamble, C., Davis, W., Pettitt, P., Richards, M., 2004. Climate Change and Evolving Human Diversity in  
659 Europe during the Last Glacial. *Philosophical Transactions of The Royal Society B Biological Sciences*  
660 359, 243-254.
- 661 Gienapp, P., Reed, T. E., Visser, M. E., 2014. Why climate change will invariably alter selection  
662 pressures on phenology. *Proceedings of the Royal Society B: Biological Sciences* 281 (1793)  
663 doi:10.1098/rspb.2014.1611.
- 664 Giorgetta, M. A., et al., 2013. Climate and carbon cycle changes from 1850 to 2100 in MPI-ESM  
665 simulations for the Coupled Model Intercomparison Project phase 5, *Journal of Advances in Modeling*  
666 *Earth Systems* 5, 572-597. Doi:10.1002/jame.20038.
- 667 Gosse, G., Varlet-Grancher, C., Bonhomme, R., Chartier, M., Allirand, J.-M., Lemaire, G., 1986.  
668 Production maximale de matière sèche et rayonnement solaire intercepté par un couvert végétal.  
669 *Agronomie* 6, 47-56.
- 670 Hassan, G. E., Youssef, M. E., Mohamed, Z. E., Ali, M. A., Hanafy, A. A., 2016. New Temperature-based  
671 Models for Predicting Global Solar Radiation. *Applied Energy* 179, 437–450.
- 672 Henderson, K., Loreau, M., 2019. An ecological theory of changing human population dynamics.  
673 *People and Nature* 1, 31-43. <https://doi.org/10.1002/pan3.8>.
- 674 Huang, W., Ge, Q., Wang, H., Dai, J. 2019. Effects of multiple climate change factors on the spring  
675 phenology of herbaceous plants in Inner Mongolia, China: Evidence from ground observation and  
676 controlled experiments. *International Journal of Climatology* 39, 5140–5153. DOI: 10.1002/joc.6131
- 677 Jiang, D., Sui, Y., Lang, X., Tian, Z., 2018. Last glacial maximum and mid-Holocene thermal growing  
678 season simulations. *Journal of Geophysical Research: Atmospheres* 123, 11,466-11,478.  
679 <https://doi.org/10.1029/2018JD028605>.
- 680 Jochim, M., 1987. Late Pleistocene refugia in Europe. In: Soffer, O. (Ed.), *The Pleistocene Old World:*  
681 *Regional Perspectives*. Plenum Press, New York, pp. 317–331.
- 682 Kaplan, J.O., Pfeiffer, M., Kolen, J.C.A., Davis, B.A.S., 2016. Large Scale Anthropogenic Reduction of  
683 Forest Cover in Last Glacial Maximum Europe. *PLoS ONE* 11(11): e0166726.  
684 doi:10.1371/journal.pone.0166726
- 685 Klein, K., Wegener, C., Schmidt, I., Rostami, M., Ludwig, P., Ulbrich, S., Weniger, G.-C., Shao, Y., in  
686 prep. Human Existence Potential in Europe during the Last Glacial Maximum.

687 Koch, P.L. , Barnosky, A.D., 2006. Late Quaternary Extinctions: State of the Debate. *Annu. Rev. Ecol.*  
688 *Evol. Syst.* 2006. 37:215–50. doi: 10.1146/annurev.ecolsys.34.011802.132415. Kretschmer, I., 2015.  
689 Demographische Untersuchungen zu Bevölkerungsdichten, Mobilität und Landnutzungsmustern im  
690 späten Jungpaläolithikum. Verlag Marie Leidorf GmbH, Rahden/Westf.

691 Krupnik, I., 2018. ‘Arctic Crashes:’ Revisiting the Human-Animal Disequilibrium Model in a Time of  
692 Rapid Change. *Human Ecology*. <https://doi.org/10.1007/s10745-018-9990-1>

693 Ludwig, P., Pinto, J. G., Raible, C. C., Shao Y., 2017. Impacts of surface boundary conditions on  
694 regional climate model simulations of European climate during the Last Glacial Maximum.  
695 *Geophysical Research Letters* 44, 5086-5095. Doi:10.1002/2017GL073622.

696 Liu, Q., Fu, Y. H., Zeng, Z., Huang, M., Li, X., Piao, S. 2016. Temperature, precipitation, and insolation  
697 effects on autumn vegetation phenology in temperate China. *Global Change Biology* (2016) 22, 644–  
698 655. <https://doi.org/10.1111/gcb.13081>

699 Maier, A., Zimmermann, A., 2017. Populations headed south? The Gravettian from a  
700 palaeodemographic point of view. *Antiquity* 91, 573-588.

701 Maier, A., Lehmkuhl, F., Ludwig, P., Melles, M., Schmidt, I., Shao, Y., Zeeden, Ch. & Zimmermann, A.,  
702 2016. Demographic estimates of hunter-gatherers during the Last Glacial Maximum in Europe against  
703 the background of palaeoenvironmental data. *Quaternary International* 425, 49-61.

704 Mandryk, C.A.S., 1993. Hunter-Gatherer Social Costs and the Nonviability of Submarginal  
705 Environments. *Journal of Anthropological Research* 49, 39-71.

706 MARGO Project Members, 2009. Constraints on the magnitude and patterns of ocean cooling at the  
707 Last Glacial Maximum, *Nature Geoscience* 2, 127–132. Doi:10.1038/ngeo411.

708 Mayor, S. Guralnick, J., R. P., Tingley, M. W., Otegui, J., Withey, J. C., Elmendorf, S. C., Andrew, M. E.,  
709 Leyk, S., Pearce, I. S., Schneider, D. C., 2017. Increasing phenological asynchrony between spring  
710 green-up and arrival of migratory birds. *Scientific Reports* 7 , 1902. doi:10.1038/s41598-017-02045-z.

711 Merkle, J. A., Monteith, K. L., Aikens, E. O., Hayes, M. M., Hersey, K. R., Middleton, A. D., Oates, B. A.,  
712 Sawyer, H., Scurlock, B. M., Kauffman, M. J., 2016. Large herbivores surf waves of green-up during  
713 spring. *Proceedings of the Royal Society B* 283. <https://doi.org/10.1098/rspb.2016.0456>.

714 Monteith, J. L., 1994. Validity of the correlation between intercepted radiation and biomass.  
715 *Agricultural and Forest Meteorology* 68, 213-220.

716 Ohlberger, J., Thackeray, S. J., Winfield, I. J., Maberly, S. C., Vøllestad, L. A., 2014. When phenology  
717 matters: Age–size truncation alters population response to trophic mismatch. *Proceedings of the*  
718 *Royal Society B: Biological Sciences* 281 (1793) doi:10.1098/rspb.2014.0938.

719 Olff, H., Ritchie, M. E., Prins, H.H.T., 2002. Global environmental controls of diversity in large  
720 herbivores. *Nature* 415, 901-904. Doi: 10.1038/415901a.

721 Pacher, M., Stuart, A. J., 2008. Extinction chronology and palaeobiology of the cave bear (*Ursus*  
722 *spelaeus*). *Boreas* 38, 189–206.

723 Parmesan, C., Hanley, M. E., 2015. Plants and climate change: Complexities and surprises. *Annals of*  
724 *Botany* 116 (6), 849–864. doi:10.1093/aob/mcv169.

725 Posth, C., Renaud, G., Mittnik, A., Drucker, D. G., Rougier, H., Cupillard, C., et al. 2016. Pleistocene  
726 mitochondrial genomes suggest a single major dispersal of Non-Africans and a Late Glacial  
727 population turnover in Europe. *Current Biology* 26, 827–833.



- 728 Roebroeks, W., 2006. The human colonization of Europe: where are we? *Journal of Quaternary*  
729 *Science* 21, 425-435.
- 730 Sandom, C., Faurby, S., Sandel, B., Svenning, J.-C., 2014. Global late Quaternary megafauna  
731 extinctions linked to humans, not climate change. *Proc. R. Soc. B* 281: 20133254.  
732 <http://dx.doi.org/10.1098/rspb.2013.3254>
- 733 Schmidt, I., Zimmermann, A., 2019. Population dynamics and socio-spatial organization of the  
734 Aurignacian: Scalable quantitative demographic data for western and central Europe. *PLoS One*  
735 14(2), e0211562.
- 736 Skamarock, W.C., Klemp, J. B., Dudhia, J., Gill, D. O., Barker, D. M., Duda, M. G., Huang, X.-Y., Wang,  
737 W., Powers, J. G., 2008. A description of the advanced research WRF version 3, NCAR Tech. Note  
738 NCAR/TN-475+STR. Doi:10.5065/D68S4MVH.
- 739 Smith, J.G.E., 1978. Economic Uncertainty in an “Original Affluent Society”: Caribou and Caribou  
740 Eater Chipewyan Adaptive Strategies. *Arctic Anthropology* 15, 68-88.
- 741 Soulier, M.-C., 2014. L’exploitation alimentaire et technique du gibier au début du Paléolithique  
742 supérieur aux Abeilles (Haute-Garonne, France). *Paleo* 25, 287-307.
- 743 Soulier, M.-C., Goutas N., Normand, C., Legarnd, A., White R., 2014. Regards croisés de  
744 l’archéozoologie et du technologue sur l’exploitation des ressources animales à l’Aurignacien  
745 archaïque : l’exemple d’Isturitz (Pyrénées-Atlantiques, France). In: Thiébault C., Claud É., Costamagno  
746 S. (eds.), *Transitions, ruptures et continuité en Préhistoire. Vol.2 : Exploitation des ressources*  
747 *organiques à la fin du Paléolithique moyen et au début du Paléolithique supérieur : interactions entre*  
748 *environnement et comportements techniques. XXVIIe congrès préhistorique de France, Bordeaux-Les*  
749 *Eyzies, 31 mai-5 juin 2010: Mémoires de la SPF, 315-332.*
- 750 Stuart, A. J., 2005. The extinction of woolly mammoth (*Mammuthus primigenius*) and straight-tusked  
751 elephant (*Palaeoloxodon antiquus*) in Europe. *Quaternary International* 126–128, 171–177.
- 752 Tallavaara, M., Luoto, M., Korhonen, N., Järvinen, H., Seppä, H., 2015. Human population dynamics in  
753 Europe over the Last Glacial Maximum. *Proceedings of the National Academy of Sciences of the*  
754 *United States of America* 112, 8232–8237.
- 755 Tallavaara, M., Eronen, J. T., Luoto, M. 2018. Productivity, biodiversity, and pathogens influence the  
756 global hunter-gatherer population density *PNAS* 115(6), 1232-1237;  
757 <https://doi.org/10.1073/pnas.1715638115>
- 758 Trugdill, D. L., Squire, G. R., Thompson, K., 2000. A thermal time basis for comparing the germination  
759 requirements of some British herbaceous plants. *New Phytology* 145, 107-114.
- 760 Van Meerbeeck, C. J., Renssen, H., Roche, D. M., 2009. How did Marine Isotope Stage 3 and Last  
761 Glacial Maximum climates differ? – Perspectives from equilibrium simulations. *Climate of the Past* 5,  
762 33–51.
- 763 Verpoorte, A., 2009. Limiting factors on early modern human dispersals: The human biogeography of  
764 late Pleniglacial Europe. *Quaternary International* 201, 77–85.
- 765 Weninger, B., Jöris, O., 2008. A 14C age calibration curve for the last 60 ka: the Greenland-Hulu U/Th  
766 timescale and its impact on understanding the Middle to Upper Paleolithic transition in Western  
767 Eurasia. *Journal of Human Evolution* 55, 772-781.

- 768 Zhang, H., Tian, Y., Zhou, D., 2018. A Modified Thermal Time Model Quantifying Germination  
769 Response to Temperature for C3 and C4 Species in Temperate Grassland. *Agriculture* 5, 412-426.  
770 Doi:10.3390/agriculture5030412.
- 771 Zickel, M., Becker, D., Verheul, J., Yener, Y., Willmes, C., 2016. Paleocoastlines GIS dataset (CRC806-  
772 Database). <https://crc806db.uni-koeln.de/maps/> accessed 02.06.2019.
- 773 Zimmermann, A., Hilpert, J., Wendt, KP., 2009. Estimations of population density for selected periods  
774 between the Neolithic and AD 1800. *Human Biology* 81, 357–380.